SAE PAPER 2019-01-0986

Engine-Aftertreatment in Closed-Loop Modeling for Heavy Duty Truck Emissions Control

Zhiming Gao, Dean Deter, David Smith, Josh Pihl, C. Stuart Daw, and James Parks
Oak Ridge National Laboratory

Citation: Gao, Z., Deter, D., Smith, D., Pihl, J. et al., "Engine-Aftertreatment in Closed-Loop Modeling for Heavy Duty Truck Emissions Control," SAE Technical Paper 2019-01-0986, 2019, doi:10.4271/2019-01-0986.

Abstract

An engine-aftertreatment computational model was developed to support in-loop performance simulations of tailpipe emissions and fuel consumption associated with a range of heavy-duty (HD) truck drive cycles. For purposes of this study, the engine-out exhaust dynamics were simulated with a combination of steady-state engine maps and dynamic correction factors that accounted for recent engine operating history. The engine correction factors were approximated as dynamic first-order lags associated with the thermal inertia of the major engine components and the rate at which engine-out exhaust temperature and composition vary as combustion heat is absorbed or lost to the surroundings. The aftertreatment model included catalytic monolith components for diesel exhaust oxidation, particulate filtration, and selective catalytic reduction of nitrogen oxides (NOx) with urea. Both the engine and aftertreatment models have been calibrated with dynamometer measurements from a commercial 2010-certificated 15-L Cummins diesel engine. The fuel consumption engine map with the reduced data is attached in the appendix. Simulations with the combined engine and aftertreatment models above appear to reveal important trends among the fuel efficiency, emissions control, power demand for HD trucks under realistic drive cycle conditions. Thus, this type of computational simulation appears to have significant value in choosing among options for HD vehicle design and operation.

Introduction

US transportation represents over 3 trillion vehicle-miles driven and 11 billion tons of freight transported annually, accounting for 70% of the nation's petroleum consumption [1]. The transportation sector also contributes over 65% of CO2, 50% of NOx, 20% of PM in the nation, which significantly impacts air pollution and climate change [1]. Heavy-duty (HD) vehicles represent only about 5 percent of total highway traffic but account for 20 percent of transportation-related fuel consumption and carbon emissions. [2]. Many nationwide fleets have shown significant interest in expending their fleet using vehicles equipped with innovative technologies, potentially improving society, environment, and economy [3]. Thus, substantial research efforts are expected to improve fuel consumption and emissions reduction in the current and future HD trucks.

Unlike light-duty (LD) vehicles, which have seen the adoption of advanced plug-in hybrid and battery electric vehicles, HD vehicles are still expected to continue using conventional diesel engines as power sources in future decades. This is because HD vehicles' requirement for extremely higher power and durability to withstand harsh working environments, which are challenging to electric vehicle technologies [4-5]. At present, nearly all HD diesel engines typically run under lean burn mode, which achieves significant higher thermal efficiency than stoichiometric gasoline engines. Moreover, the HD diesel engines are expected to continue the efficiency improvement in future. For example, the US DOE's SuperTruck program with 15 industry partners (including six truck manufacturers) already developed 50% braking thermal efficiency in demonstration truck and aims to demonstrate engines having thermal efficiency of 55% by 2021 [6]. However, advanced lean diesel engine technologies bring a substantial challenge for emissions control which requires complex and expensive exhaust aftertreatment systems, particularly for NOx and PM emissions control [7-9]. Advanced combustion efficiency improvements lower engine exhaust temperature considerably, and hamper the performance of lean exhaust aftertreatment devices [10].

On the other hand, HD vehicle emissions regulations are becoming more and more restrictive (see Figure 1). For example, the US EPA 2010 emission standards for heavy-duty engines have established a limit for oxides of nitrogen (NOx) emissions of 0.20 g/bhp-hr, a 90% reduction from the previous emission standards. Furthermore, California ARB required manufacturers to achieve NOx emissions significantly lower than the current engine standard. The target NOx emission rate of California ARB over the heavy-duty Federal Test Procedure (FTP) is 0.02 g/bhp-hr [11]. To achieve such extremely challenging targets, it is necessary to carry out significant co-optimization between HD diesel engine and lean exhaust aftertreatment systems in future HD conditions. This makes successful computational simulation of emissions and fuel efficiency performance extremely important in co-optimization of engine and emissions control technologies. Specifically, the engine model must accurately reflect the complex transients in fuel consumption and engine-out exhaust temperature and composition that occur during realistic driving conditions. Likewise, the response of the aftertreatment system to these transient inputs should be able to accurately reflect the resulting impact on tailpipe emissions of regulated species. As far as we are aware, there is a significant lack of readily available, calibrated computational tools to enable simulations of how such aftertreatment components should respond to realistic variations in HD engine-out exhaust under realistic drive cycles.

Our objective in this study, therefore, is to develop and demonstrate an engine-aftertreatment computational approach that can be used to simulate the effects of different combinations of component models and also as a starting point for use in hardware-in-the-loop (HIL)

testing. Our component models are based on Oak Ridge National Laboratory (ORNL) in-house component models that have been successfully used to represent an experimentally studied HD engine and commercial aftertreatment catalysts. We expect that this approach can be extended to simulations where hardware components and/or other commercially available or user-defined component models are included (e.g. in Autonomie [12]). For demonstration here, the HD truck is assumed to include a 15-L diesel engine ((engine rated power: 336kW)) and its aftertreatment DOC/CDPF/SCR system operating over short and long-haul real-road driving cycles.

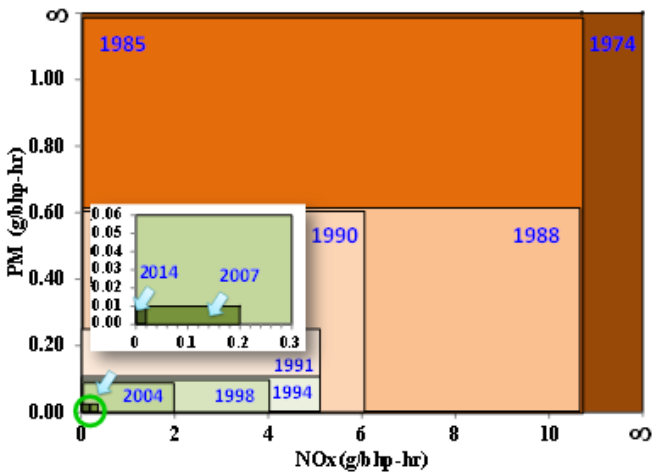

Figure 1. US EPA regulation history for highway HD engines (data source: [13]). The 2014 is California ARB data and others are EPA data.

Engine and aftertreatment model approach

We used the following simplified dynamic engine model to approximate transient fuel consumption and engine-out exhaust temperature and composition in combination with three specific types of exhaust after-treatment component models: a diesel oxidation catalyst (DOC), a selective catalytic reduction monolith (SCR), and a catalyzed diesel particulate filter (DPF).

Transient engine model

Aftertreatment performance depends critically on engine-out exhaust temperature and composition. The key chemical reaction rates vary exponentially with temperature and also depend on species concentrations. Thus it is critical to accurately predict the transient engine-out exhaust properties as functions of speed, load, and previous history (e.g. exhaust composition and temperature during cold-start and start–stop transients). Experimental steady-state performance maps have previously been used to relate engine-out exhaust temperatures and species with engine speed and load, but this approach is not capable of capturing the hysteretic effects associated with cold-start, start/stop and other complex speed and load transients occurring during typical driving conditions. To account for these hysteretic effects, we reported a simple strategy described in detail elsewhere [14]. Briefly, this approach assumes that instantaneous engine-out exhaust temperature and emissions can be estimated by applying dynamic correction factors to steady-state engine maps and limited transient engine data as outlined in Figure 2. The correction factors are modeled as dynamic first-order lags associated with a warm-up index determined from the global heat balance on the engine. Lag parameters are estimated from experimental measurements or based on known engine characteristics. Given a set of initial engine conditions and drive cycle profile, it is thus possible to estimate the variations in engine-out exhaust temperature and emissions over time.

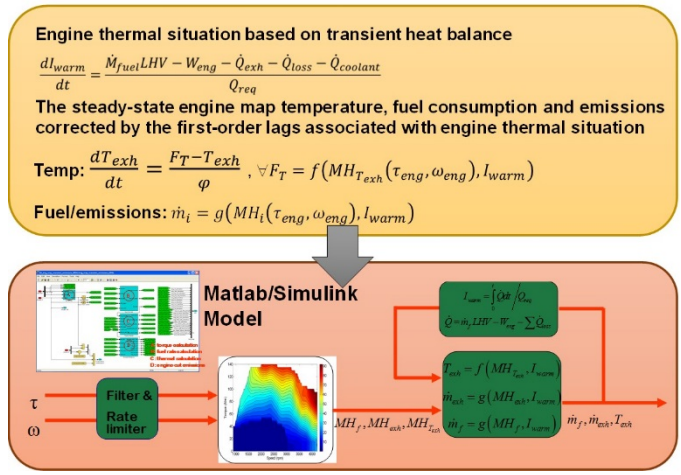

Figure 2. The methodology of map-based engine adjusted for transient performance over cold-starts and stop-restarts [14].

The DOC component model

Diesel oxidation catalysts oxidize unburned hydrocarbons (HCs) and carbon monoxide (CO) in lean exhaust. In modern after-treatment assemblies, DOCs are often located upstream of NOx and particulate control devices so that the catalyst can also oxidize NO in the engine exhaust to NO_2, improving the efficiency of the NOx and particulate removal steps. Our DOC model used here considers three global one-step reactions, including CO oxidation, HC oxidation, and NO oxidation. We assume that the global performance of the DOC device can be approximated by a single, representative one-dimensional channel with transient plug flow. All reactions are assumed to occur in the washcoat. A full-developed laminar flow is assumed for heat and mass transfer between gaseous and solid-phase species. All hydrocarbons are represented by equimolar concentrations of propylene (C_3H_6). In addition to transient species balances, the DOC model also includes a differential energy balance to track axial and temporal temperature variations. The effects of initial conditions, engine-out temperature and species variations, and ambient heat loss are all included in the boundary conditions. The details are provided in Figure 3 or see [15]. The kinetic parameters used for the three reaction rates were based on typical literature values and adjusted slightly to match the testing data reported by Triana [16] and ORNL data [17] for Johnson Matthey and EmeraChem DOC products, respectively.

$$\frac{\partial x_{g_i}}{\partial t} + u_g \frac{\partial x_{g_i}}{\partial z} = \frac{h_m G_m}{\varepsilon}\left(x_{s_i} - x_{g_i}\right)$$

$$\frac{\partial x_{s_i}}{\partial t} = \frac{h_m G_m}{\varepsilon(1-\varepsilon)}\left(x_{g_i} - x_{s_i}\right) + \frac{1}{\rho_m \varepsilon(1-\varepsilon)}\sum_k \alpha_i^k R^k$$

$$\rho_g c_{pg} \varepsilon\left(\frac{\partial T_g}{\partial t} + u_g \frac{\partial T_g}{\partial z}\right) = h_g G_m \left(T_s - T_g\right)$$

$$\rho_s c_{ps}(1-\varepsilon)\frac{\partial T_s}{\partial t} = k_s(1-\varepsilon)\frac{\partial^2 T_s}{\partial z^2} + h_g G_m\left(T_g - T_s\right) + h_a G_a\left(T_a - T_s\right) + \sum_{k=1}^{n} R^k \cdot \Delta H^k$$

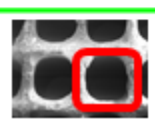

$$CO + 1/2\,O_2 \Rightarrow CO_2 + \Delta H_{CO-O_2}$$
$$C_3H_6 + 9/2\,O_2 \Rightarrow 3CO_2 + 3H_2O + \Delta H_{C_3H_6-O_2}$$
$$NO + 1/2\,O_2 \Leftrightarrow NO_2 + \Delta H_{NO-O_2}$$

Figure 3. The 1-D transient differential balances and reaction mechanism considered in the DOC component model [15].

The SCR component model

The SCR component model also utilizes 1-D differential transient balances similar to the above DOC model. It is assumed that the rate limiting steps in the SCR device occur after urea is converted to NH_3, thus the model does not account for vaporization and thermolysis of the urea slurry. Since SCR technology is still rapidly evolving, three SCR models were developed for commercial Cu-ZSM-5, chabazite Cu-zeolite and Cu-SSZ-13, respectively. All these models account for three main global catalytic reactions: (1) the standard reaction between NH_3 and NO; (2) the fast reaction between NH_3 and equimolar levels of NO and NO_2; and (3) the reaction between NH_3 and NO_2. Details of the SCR models are summarized in Table 1. As mentioned earlier, SCR technology is still rapidly evolving. It is likely that urea injection strategies and catalyst parameter values will continue to improve as more advanced catalytic materials are developed and more understanding is gained about their functionality. Therefore, in this study, we assumed a simple urea injection strategy such that the instantaneous urea rate was always adjusted to produce the optimal stoichiometric ratio of NH_3 to NO at the SCR catalyst inlet when the inlet temperature was above 150°C. For lower temperatures, urea injection was stopped.

Table 1. Three SCR models for Cu-ZSM-5 [15], commercial chabazite Cu-zeolite [18] and Cu-SSZ-13 [19].

Material	Cu-ZSM-5	Cu-chabazite	Cu-SSZ-13
Storage site	Single site	Single site	Two sites
Adsorption reactions	NH_3 adsorption	NH_3 adsorption	NH_3/H_2O adsorption
Surface reactions	NH_3/NO oxidation, Std SCR, Fast SCR, NO_2 SCR	NH_3/NO oxidation, Std SCR, Fast SCR, NO_2 SCR	NH_3/NO oxidation, Std SCR, Fast SCR, NO_2 SCR, N_2O formation, NH_3-nitrate formation
Gas-phase reactions	N/A	NH_3 oxidation, Std SCR, Fast SCR, NO_2 SCR	N/A

The DPF component model

Catalyzed diesel particulate filters (CDPFs) remove particulates from engine exhaust by mechanical filtration and subsequently oxidize the solid carbon and residual HCs. Adequate oxidation of the particulate is necessary to prevent buildup of back pressure, which penalizes engine output. Some degree of PM oxidation is always occurring, but the rate is an exponential function of local temperature in the DPF. So in cases where PM oxidation rates are low, it is necessary to occasionally stimulate PM oxidation by burning extra fuel to raise the engine-out exhaust temperature. This is referred to as active DPF regeneration. Thus accurate simulation of the accumulated DPF soot levels is important for determining fuel economy. Here a simplified 3-zone catalytic DPF model was used to approximate the catalyzed DPF as a combination of an inlet channel zone, an outlet channel zone, and a filter wall. Temperature can vary from zone to zone but is assumed to be uniform within each zone. Deposited PM is considered to effectively include two layers: a deeper layer in close proximity to the catalyst and an outer bulk soot cake (see Figure 4). DPF wall Filtration model is based on a collection of spherical ''unit collector'' (see Figure 4). In the CDPF model, PM oxidation by O_2 and NO_2 is considered in the cake layer without any catalytic acceleration, while considered oxidation by O_2 is catalytically accelerated in the deeper layer. Details of the global oxidation kinetics parameters have been published elsewhere [20]. We also included one-step reactions in the deep layer for oxidation of CO, HCs, and NO. Except for catalyst loading, the kinetic parameters for these oxidation reactions are assumed to be identical to those in the DOC model described above. The active DPF regeneration is considered in the engine-aftertreatment in closed-loop integration based on the assumption that active DPF regeneration would only be required when the engine-out back pressure reached a specified threshold.

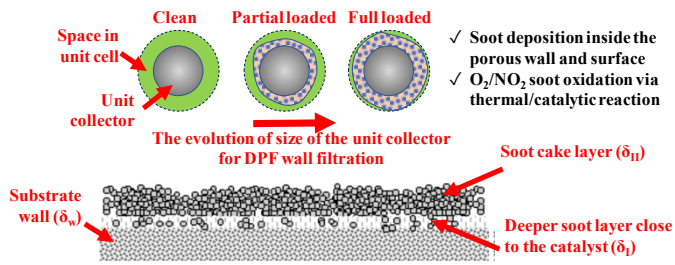

Figure 4. DPF filtration submodel used in the three-zone CDPF model accounting for the inlet channel, outlet channel, and filter wall zones [20].

Engine and aftertreatment in closed-loop integration

The integration of engine-aftertreatment in closed-loop modeling was established based on the engine and aftertreatment models discussed above. The modeling loop were developed into special Matlab/Simulink modules which can be implemented into any commercial vehicle simulation platform (e.g. Autonomie) to carry out software in loop or hardware in loop for any HD truck powertrain systems (see Figure 5) [21]. Moreover, the Matlab/Simulink modules can be used to study both conventional and hybrid electric vehicles for both LD/HD vehicles. In addition, the CPU computing timing of the modules is 20 time faster than real-time.

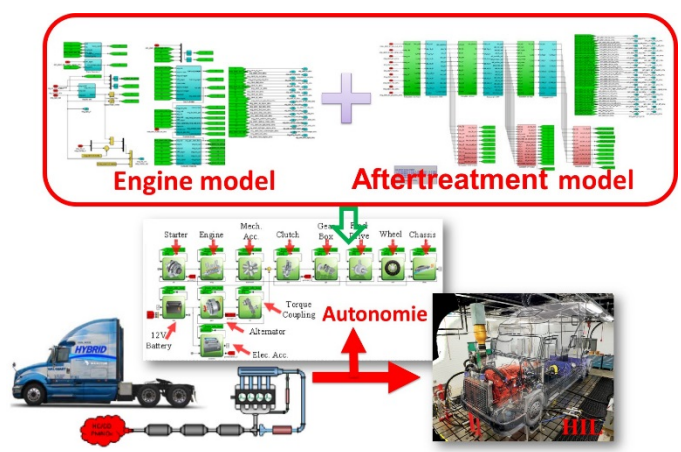

Figure 5. The configuration of engine-aftertreatment in loop integration and its application examples to software in loop or hardware in loop.

In the integration, active DPF regeneration was established between engine and DPF models. As mentioned earlier, the active DPF regeneration would only be triggered when the engine-out back pressure reached a specified threshold. Under these circumstances, active regeneration is accomplished by changing engine combustion mode via adding extra fuel to raise the exhaust temperature and stimulate accumulated PM oxidation. Otherwise, passive regeneration (where no extra fuel is needed) can occur when engine out

temperatures are sufficiently high to promote spontaneous PM oxidation.

HD drive cycle simulations

We utilized the transient and steady state data measured from a 2010-certificated 15-L Cummins diesel engine and aftertreatment components at ORNL vehicle system integration (VSI) lab to generate engine maps and validate the engine-aftertreatment modeling in closed-loop. The aftertreatment system comprises a 5.8-L DOC, a 19-L catalyzed DPF, and a 24-L SCR catalyst. The integrated engine and aftertreatment assembly system are shown in Figure 6(a). Three groups of engine data have been measured, including engine maximum torque curves, steady-state engine performance data, and transient engine performance data operating over heavy-duty FTP cycles. The FTP cycle takes a running time of 1200s and account for a variety of heavy-duty truck and bus driving patterns in American cities [22]. The average load factor of the FTP cycle is roughly 20-25% of the maximum engine power available at a given engine speed. The normalized speed and torque with time is shown in Figure 6(b). Figure 6(c) displays the tested engine speed and torque profiles of the 15-L diesel engine according to the normalized speed and torque requested in FTP.

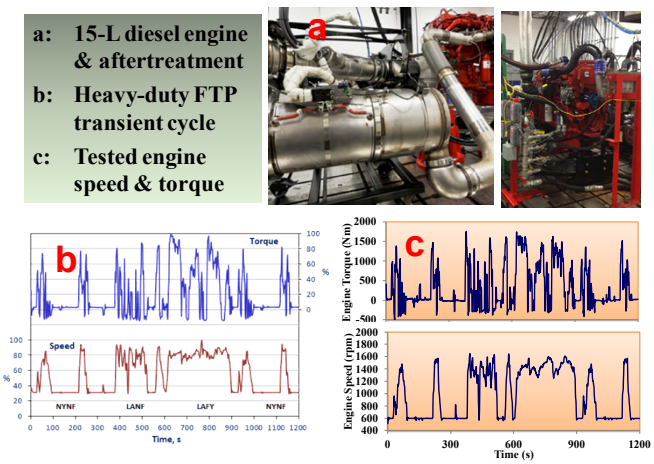

Figure 6. (a) A 2010-certificated 15-L Cummins engine, (b) heavy-duty FTP transient cycle and (c) the tested engine speed and torque profiles.

We used both the maximum torque curves and steady-state data to create comprehensive engine maps which account for fuel consumption, exhaust temperature, and engine-out emissions. Figure 7 depicts example plots of the steady-state engine map for efficiency, exhaust temperature and engine-out NOx emissions. The peak efficiency of the engine is around 45%. In these figures, the red markers represent the measured engine operating points within the performance map, covering a range from 620 to 2100 rpm with up to 2200 Nm maximum torque. The fuel consumption engine map with the reduced data is attached in the appendix section. The steady-state engine performance maps have been implemented into our transient engine model to proficiently and accurately simulate power and exhaust characteristics of advanced HD diesel engines operation. Unlike the first two group data, the FTP transient data encompass engine-out exhaust properties and aftertreatment device (i.e. DOC/DPF/SCR) tailpipe emissions. The data were used to calibrate and validate our transient HD engine and aftertreatment component models.

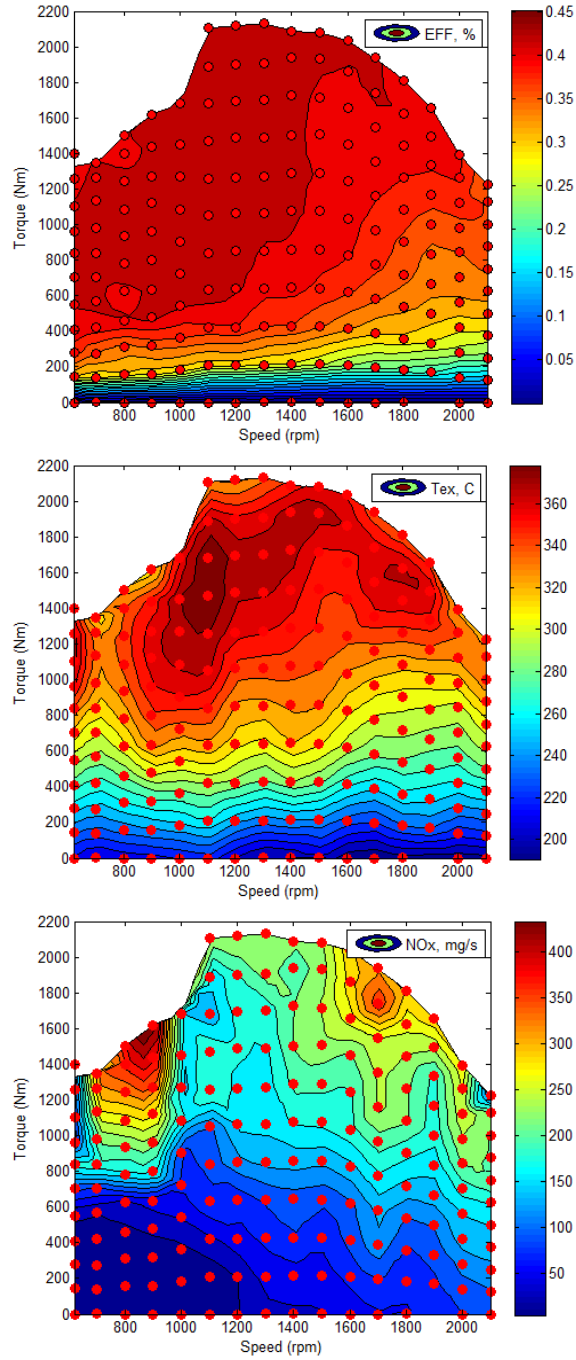

Figure 7. The steady-state engine map for engine efficiency, exhaust temperature and engine-out NOx emissions using ORNL VSI lab data measured at a 2010-certifcated HD 15-L Cummins engine.

Table 2 summarizes the predicted cumulative engine-out emissions and fuel consumption with the experimental measurements. Most of the prediction errors are less than 5%, particularly for hot start cases. However, the modeled THC and NOx emissions during the cold start cycle are significantly higher than the experimental results. We conjecture that the major reason could be impact of cold-start which makes a completely different combustion mechanism compared to hot-start cases. The steady-state engine performance maps could have constraints in predicting THC and NOx emissions, especially during a cold-start. The engine runs at 20°C at the beginning in the cold-start cases, while the hot-start cases typically reruns engine with a ten-minute engine-off after completing a previous FTP cycle.

Table 2. Comparison of predicted cumulative engine-out emissions and fuel consumption with the experimental measurements.

Fuel/ engine-out emission	Cold-start		Hot start	
	Measured	Simulated	Measured	Simulated
Fuel (kg)	4.34	4.12	4.03	3.96
CO (g)	12.00	11.44	9.47	9.93
THC (g)	5.66	6.78	6.70	6.73
NOx (g)	59.66	73.33	69.31	73.71
CO2 (g)	14.10	13.55	13.07	13.28
O2 (kg)	25.14	25.76	25.60	25.51
Exh (kg)	174.36	171.41	170.74	169.46

Figures 8 and 9 compare the resulting fuel consumption and exhaust temperature predictions with the measurements for both cold and hot start FTP cycles, respectively. The observations demonstrate that the transient engine model is reasonably well able to predict the transient fuel consumption and exhaust temperature variation. The latter is fairly important to the downstream aftertreatment component models in order to achieve accurate tailpipe emissions control. Based on Table 2 and Figures 8-9, we conclude that our transient engine model is fairly consistent to predict HD engine fuel consumption and exhaust properties including temperature, as was also reflected in our previous results for LD gasoline and diesel engines [14].

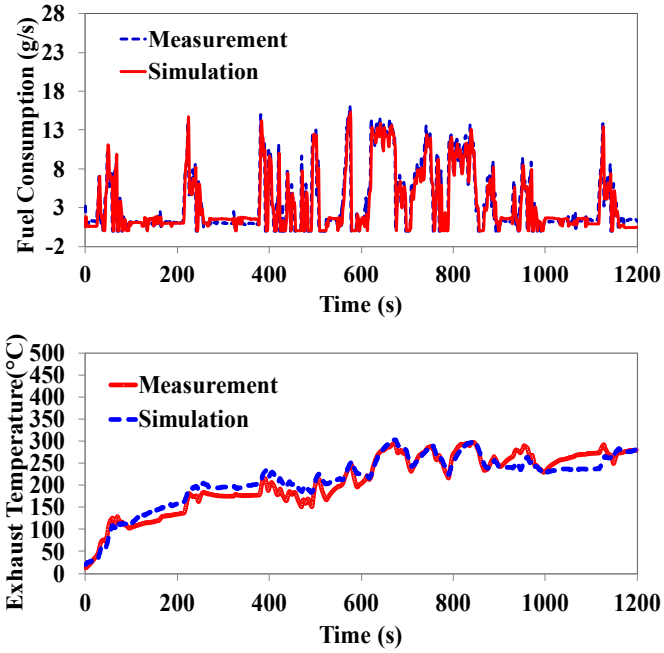

Figure 8. Comparison of the fuel consumption and exhaust temperature between the prediction and measurement over the cold-start HD FTP cycle.

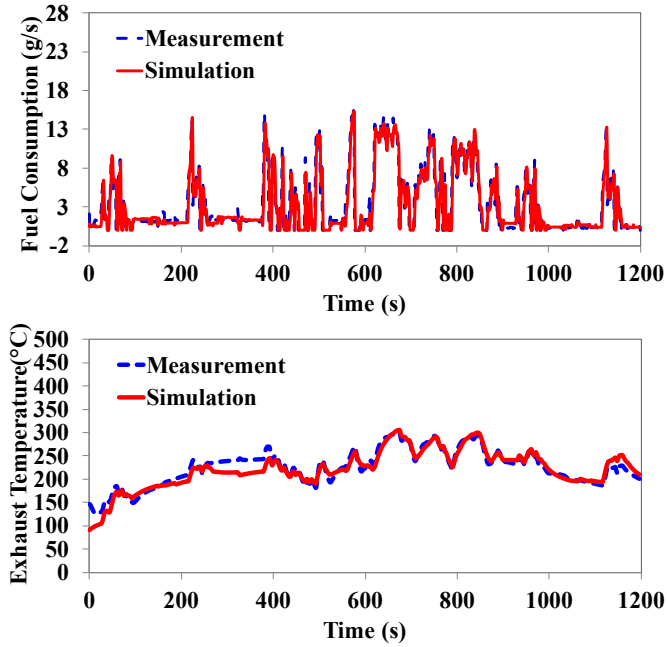

Figure 9. Comparison of the fuel consumption and exhaust temperature between the prediction and measurement over the hot-start HD FTP cycle.

Table 3 shows the results of predicted and measured cumulative CO/THC/NOx tailpipe emissions over the HD FTP cycles. For the cold-start case, all the predicted tailpipe emissions are reasonably close to the measurements, not more than 6%. Figure 10 shows transient CO/THC/NOx emissions at a 1s interval, which demonstrates a reasonably simulated trend in a 20°C transient cold-start. For the hot-start case, the predicted errors for CO and THC are more than 70-85% compared to the tested data while the predicted error of NOx emissions is 8%. The main reason is that, in the hot-start case, the net emissions are actually very low so that a tiny difference could cause a remarkable error. In fact, the predicted CO/HC oxidation efficiencies are very reasonably close to the measurements in the hot-start case (see Table 3).

Table 3. Comparisons of predicted and measured cumulative tailpipe emissions over cold- and hot-start HD FTP cycles.

Tailpipe Emission	Cold-start		Hot start	
	Measured	Simulated	Measured	Simulated
CO (g)	0.47	0.48	0.02	0.03
CO eff	96%	96%	99.8%	99.7%
THC (g)	0.39	0.37	0.16	0.02
THC eff	93.2%	93.6%	97.5%	99.6%
NOx (g)	27.79	27.22	8.20	8.85
NOx eff	53.4%	54.4%	86.4%	85.3%

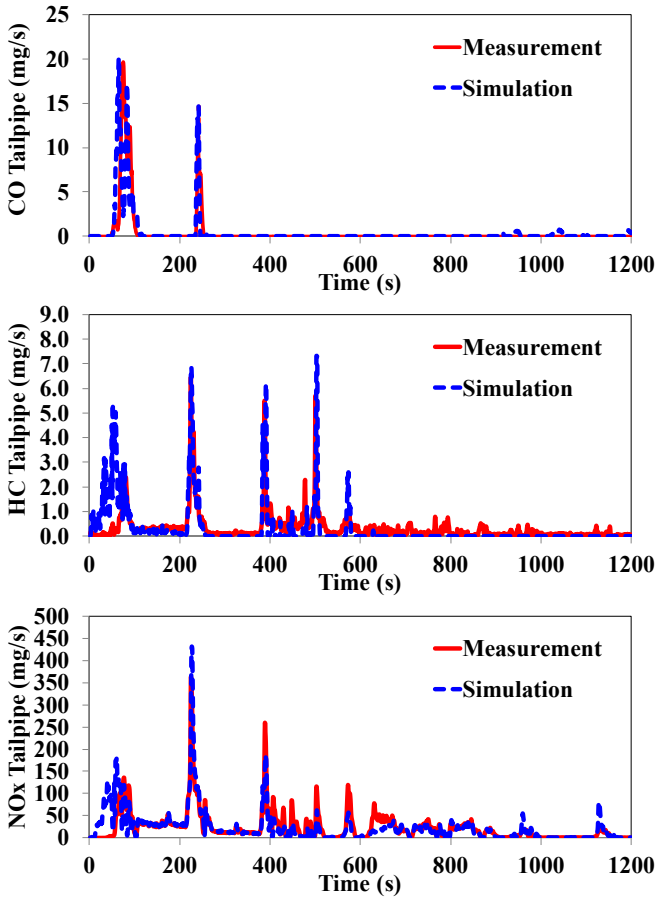

Figure 10. Comparison of predicted and measured CO/THC/NOx tailpipe emissions of the 2010 15-L Cummins diesel engine with DOC/CDPF/SCR aftertreatment system over a cold-start HD FTP transient cycle.

Figures 11 and 12 plot the predicted and measured catalyst-out exhaust temperature and DPF preesure drop over the cold-start and hot-start HD FTP transient cycles, respectively. Although the measurement system did not provide these catalyst internal temperatures, the comparison of predicted and measured catalyst-out exhaust temperatures could still reflect the capability of the current aftertreatment model in predicting their performance very well in accuracy, particularly in reflecting the transient thermal conditions of these catalysts. The transient thermal conditions are important to simulate the kinetic reaction performance of these catalysts. Also, Figures 11 and 12 show a good agreement of the transient predicted and measured pressure drop within the equipped DPF. The result exhibits the sufficient capability of our DPF model in reflecting actual DPF pressure drop performance. DPF pressure drop could cause higher engine back pressure, leading to substantial engine fuel penalty. Thus, the precise prediction of DPF pressure drop is vital to evaluate fuel economy and emissions control of HD trucks equipped with DPF device. In general, the aftertreatment component models described here appear to be capable of providing useful insights and can play an important role for assessing different engine and aftertreatment in loop optimization in order to accomplish HD drive-cycle emissions control and fuel saving goals.

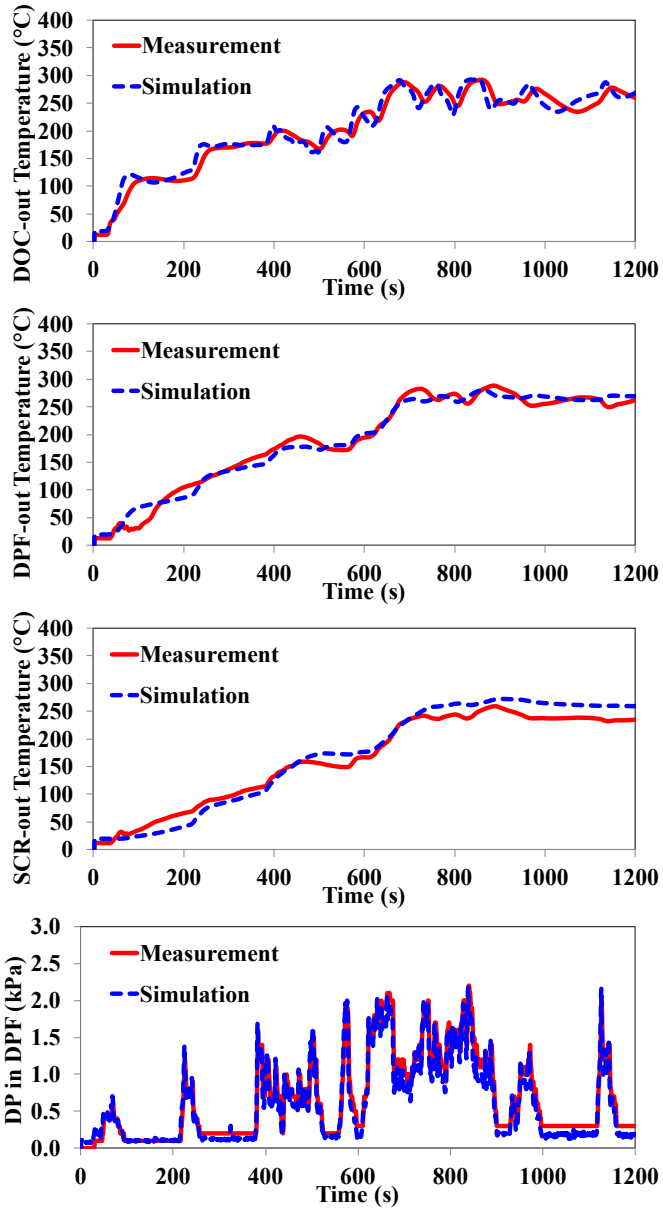

Figure 11. Comparison of predicted and measured catalyst-out exhaust temperature and DPF preesure drop of the 2010 15-L Cummins diesel engine equipped with DOC/CDPF/SCR aftertreatment system over a cold-start HD FTP transient cycle.

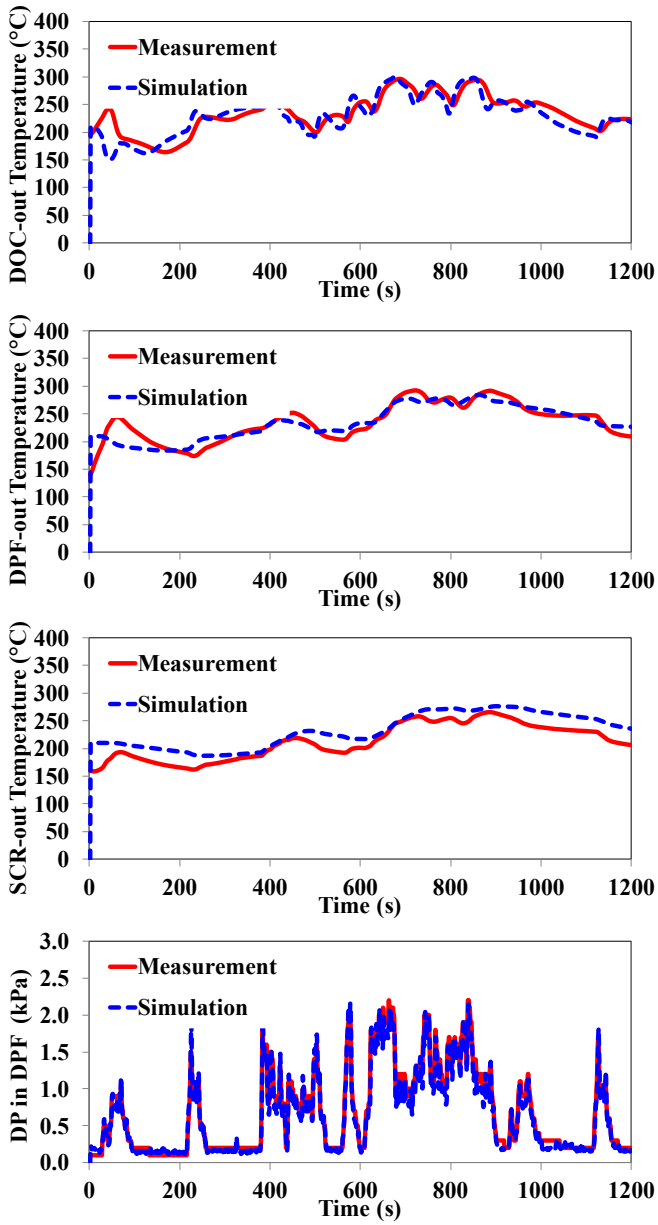

Figure 12. Comparison of predicted and measured catalyst-out exhaust temperature and DPF pressure drop of the 2010 15-L Cummins diesel engine equipped with DOC/CDPF/SCR aftertreatment system over a hot-start HD FTP transient cycle.

Modeling in closed-loop application for advanced HD powertrains

In demonstrating the modeling in-loop application for HD powertrains, a conventional Class 8 truck configuration was specified using Autonomie. This truck configuration was based on the authors' previous truck model developed for a Class 8 truck [23, 24]. The previous conventional truck model has been validated well against the experimental data measured from a 2005 Volvo tractor powered by the 2004 Cummins diesel engine at West Virginia University (WVU) [23, 24]. The predicted and measured fuel economies were 4.55 mpg vs. 4.63 mpg, respectively, for a measured urban dynamometer driving schedule truck cycle.

In the current studies, the new conventional HD Autonomie truck was updated to be powered by the 2010-certificated, Cummins 15-L, 6-cylinder diesel engine and a 10-speed manual transmission. The key vehicle parameters include rolling resistance coefficient is 0.007 and aerodynamic drag coefficient is 0.58. The simulated truck weight is 65000 lb. For the more detailed specifications of the baseline Class 8 conventional truck, see our previous literature [23, 24].

To evaluate the emissions control of long-haul trucks over real road conditions, a freeway-dominant heavy-duty truck (FDHDT) driving cycle from Knoxville to Nashville was selected from ORNL duty cycle database [23, 24]. The drive cycle was measured during normal operations from Class 8 tractor trailers in a fleet engaged in freight delivery. The FDHDT covers 196.4 mi in 3.72 h and includes significant grades (see Figure 13). The cycle is dominated by highway operating conditions, but it also contains considerable idling and limited city driving conditions. Specifically, the cycle consists of 12%, 13%, and 75% time for idle condition, for 0 to 50 mph, and for above 50 mph, respectively. Such a cycle has been found to be rather typical of highway dominant trucking operations, and the driving cycle is able to reasonably reflect the impact of real road conditions on Class 8 long-haul truck fuel consumption and emissions.

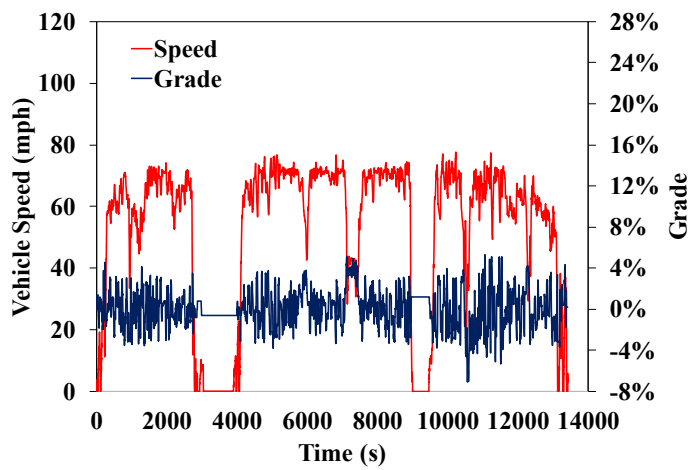

Figure 13. Speed profile of the simulated freeway-dominated heavy-duty truck driving cycle with real grade [23].

Figure 14 displays emissions transients in the simulated conventional baseline case. The major CO and HC emissions are oxidized through DOC, and then further reduced in the following catalyzed DPF which is also capable of CO and HC oxidation. For CO and HC tailpipe emissions, their reductions are more than 99%. For NOx tailpipe emissions, SCR achieves slightly less than 80% of NOx reduction. Meanwhile, the results show that the truck idle time located at the period of 3000s-4000s and 9000s-9500s still achieves a fairly good CO/HC/NOx reduction. Figure 15 shows that the 2010 certificated engine exhaust and catalysts temperature during idling can reach 200°C, which is a typical light-off temperature for CO/HC/NOx reduction.

Moreover, we simulated the transient details of the simulated conventional truck powered by 2004, 2007, and 2010 Cummins 15-L engines. Figure 16 shows an example of exhaust temperature for these engines in the above conventional truck simulation. Compared to 2004 and 2007 Cummins 15-L diesel engines, the results show that this 2010-certificated diesel engine is capable of achieving better engine efficiency and low engine-out PM emissions with the penalty of higher NOx emissions and lower exhaust temperature during loading, as

reflects the current engine technology trend is more reliant on advanced aftertreatment for improved fuel economy. Although we observe that the 2010 engine achieves a lower exhaust temperature during loading (see Figure 16), the idle temperature of the 2010 engine is close to 200°C, as is probably designated to satisfy 2010 emissions regulation.

For PM emissions, PM layer in the catalyzed DPF keeps fairly a constant level, which means that PM emissions are continuously oxidized in the catalyzed DPF. This is mainly due to the fact that the majority of exhaust temperature is between 250°C and 300°C, which is a typical temperature for catalyzed DPF passive regeneration. Such continuous and passive DPF regeneration could reduce fuel penalty relative to the proactive regeneration events. Since the rates of PM accumulation in the DPF is still sufficiently low to keep below the back pressure threshold during the drive cycles, our models do not trigger active regeneration, shown in Figure 15. Future studies may consider multi-cycle periods in order to address the impacts of active regeneration.

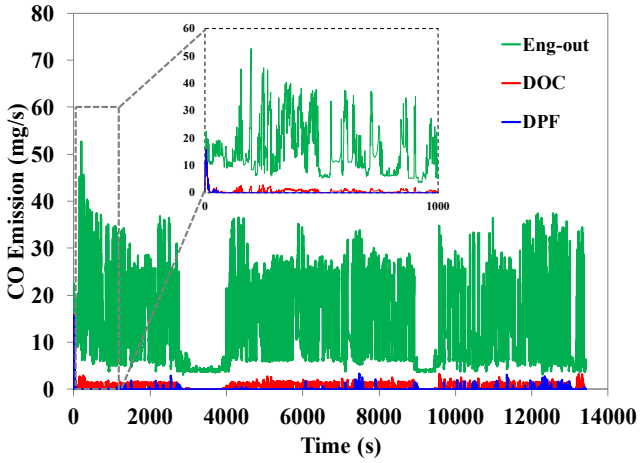

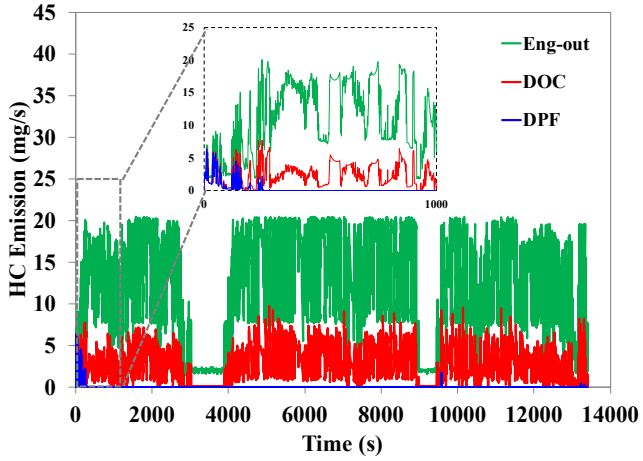

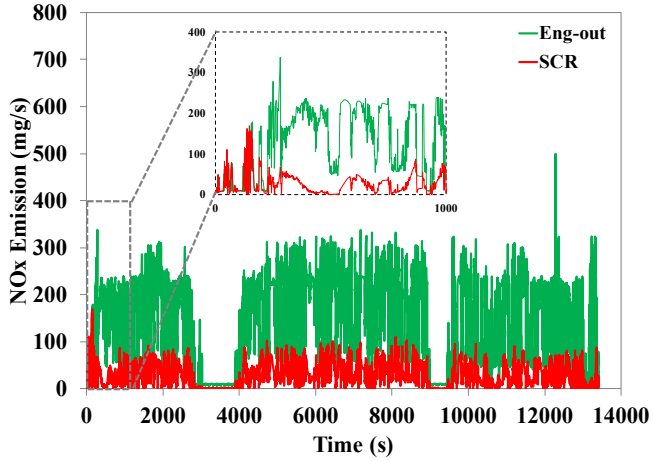

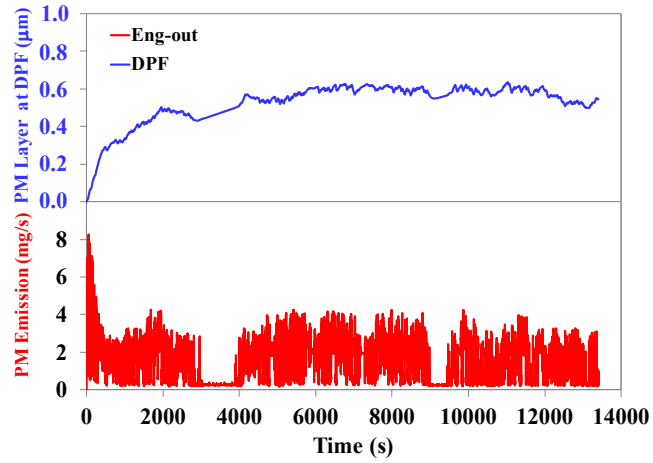

Figure 14. Emissions transients in the simulated conventional Class 8 long-haul tractor powered by the 2010 15-L Cummins diesel engine integrated with DOC/CDPF/SCR aftertreatment system over the cold-start FDHDT. Truck weight is 65000 lb.

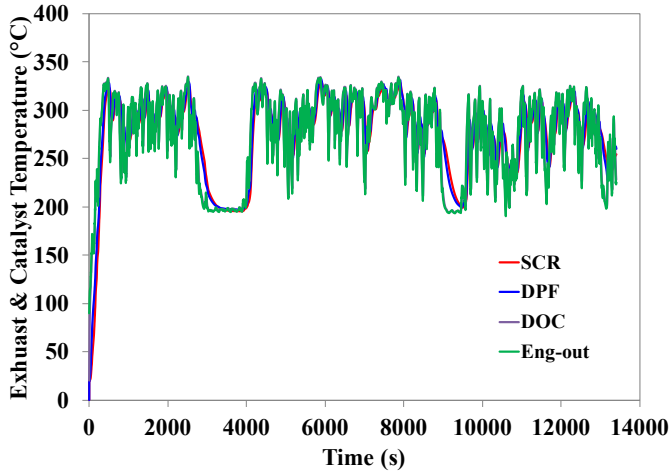

Figure 15. Simulated engine exhaust and DOC/DPF/SCR temperature transient in the conventional Class 8 long-haul tractor powered by 2010 certificated engines, respectively, over the FDHDT. Truck weight is 65000 lb.

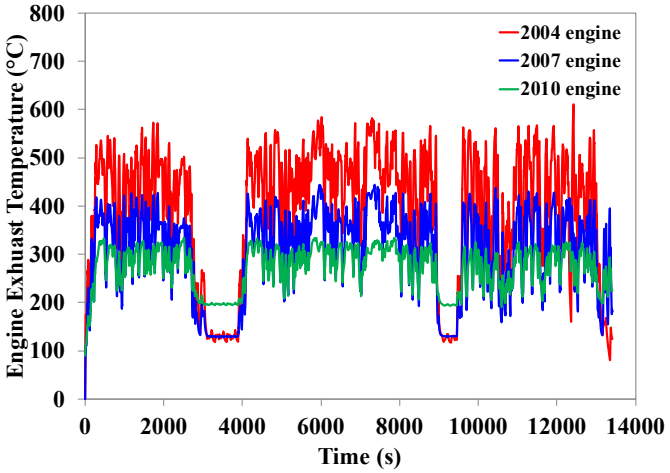

Figure 16. Simulated engine exhaust temperature transients in the conventional Class 8 long-haul tractor powered by 2004, 2007 and 2010 certificated engines, respectively, over the FDHDT. Truck weight is 65000 lb.

We included aerodynamic drag and rolling resistance in our additional simulations, as well as engine downsizing, on conventional and hybrid long-haul trucks. The hybrid powertrain configuration used is a pre-transmission parallel configuration with a sustainable charge control strategy, which has been reported in our previous literature [23, 24]. In the studies, we considered aggressive 35% rolling resistance reduction and 35-54% aerodynamic drag reduction, while engine downsizing is 15%. Based on the 65000 lb conventional truck baseline weight, the mass penalties relative to extra device for hybridization and lower aerodynamic drag and rolling resistance were added in the appropriate simulations. The simulated results are summarized in Table 4. The observations show aerodynamic drag and rolling resistance reductions are capable of increasing fuel economy due to load reduction significantly. Hybridization improves the long-haul truck fuel economy due to better engine efficiencies, particularly with the aggressive aerodynamic drag and rolling resistance reductions. Under the condition of aggressive aerodynamic drag and rolling resistance reductions, engine downsizing become possible due to significant load reduction, and achieves 1.7% fuel economy benefit in the simulated case. In summary, lower aerodynamic drag and rolling resistance technologies enable to reduce truck heavy power demand or shift heavy power demand to lower level. This particularly benefits hybridization and engine downsizing.

Table 4 also shows emissions control in the simulated long-haul trucks. Obviously, load reductions decrease engine-out CO/HC/NOx emissions. As expected, hybridization and engine downsizing are capable of further reducing the level of engine-out emissions. However, tailpipe emissions demonstrate different phenomenon. For CO and HC tailpipe emissions, their reductions are up to 99%. Thus the impact of aerodynamic drag and rolling resistance, engine downsizing, as well as hybridization is limited so that the tailpipe CO and HC emissions in the simulated cases are very close. For NOx tailpipe emissions, aerodynamic drag and rolling resistance reductions could still benefit NOx reduction, but hybridization could increase NOx slightly.

Table 4. Summary of aerodynamic drag, rolling resistance, and engine downsizing on fuel economy, efficiency and emissions of conventional and hybrid long-haul trucks over the FDHDT.

Case	Eng Eff (%)	FE (MPG)	Eng-CO (g/mile)	Eng-HC (g/mile)	Eng-NOx (g/mile)	Eng-PM (g/mile)	Tail-CO (g/mile)	Tail-HC (g/mile)	Tail-NOx (g/mile)	Tail-PM (g/mile)
Conv_Base	41.1%	5.264	0.9048	0.8030	9.8248	0.1039	0.0048	0.0016	2.1043	0.0003
Conv_Crr_35%cut	40.5%	5.739	0.8641	0.7705	9.1785	0.0979	0.0044	0.0016	1.9341	0.0002
Conv_Cd_30%cut	40.3%	5.882	0.8510	0.7604	8.9862	0.0959	0.0043	0.0016	1.8666	0.0002
Conv_Cd_54%cut	39.7%	6.442	0.8034	0.7254	8.3662	0.0897	0.0041	0.0016	1.6925	0.0002
Conv_Crr_35%cut_Cd_30%cut	39.7%	6.455	0.8075	0.7261	8.3533	0.0898	0.0040	0.0017	1.7093	0.0002
Conv_Crr_35%cut_Cd_54%cut	39.0%	7.069	0.7602	0.6915	7.7936	0.0841	0.0043	0.0017	1.4435	0.0002
Hev_Base	42.5%	5.547	0.8467	0.7011	9.2217	0.1039	0.0046	0.0018	2.1360	0.0003
Hev_Crr_35%cut_Cd_30%cut	41.8%	7.480	0.7303	0.5449	7.0571	0.0909	0.0046	0.0018	1.6914	0.0002
Hev_Crr_35%cut_Cd_54%cut	41.3%	8.536	0.6911	0.4889	6.2800	0.0862	0.0052	0.0022	1.4612	0.0002
Hev_Crr_35%cut_Cd_30%cut_Size_15%cut	42.1%	8.802	0.6102	0.4473	5.8750	0.0772	0.0048	0.0015	1.4494	0.0001

Conv_base & HEV_base : Crr=0.007; Cd=0.58; engine size=15 Liter

Crr_35%cut : 35% les than Crr=0.007; Cd_30%cut : 30% less than Cd=0.58; Size_15%cut: engine size lessn than 15L

Conclusions

Based on our observations in studying a comprehensive combination of engine and aftertreatment component computational models for simulating HD truck drive cycle performance trends, we conclude that such an approach is useful for demonstrating the effects of variations in system design and operation on fuel consumption and emissions controls performance. It is possible to calibrate a simplified engine component model with steady-state dynamometer measurements to represent recent commercial HD diesel engines and then add dynamic correction factors to account for recent engine history. Aftertreatment assembly components, such as DOCs, DPFs and SCRs, can be effectively represented with transient 1D integral reactor models. We expect the same methodology could also be used to include the effects of other aftertreatment components such as lean NOx traps (LNTs) and hydrocarbon traps (HCTs) to evaluate how to meet future emissions regulation targets.

Therefore, based on these results, we conclude that similar computational simulations with relatively simple engine and aftertreatment component models can be used to assess a wide range of technology options for optimizing both the fuel consumption and emissions control of HD trucks operating over realistic drive cycles, including complex cycles with varying engine size, cold start, large speed and load transients, varying aerodynamic drag and rolling resistance characteristics, and hybridization. Because of the rapid simulation speed of such models, we also expect that they can be readily utilized in combination with actual component hardware for HIL studies.

References

1. https://www.energy.gov/eere/vehicles/about-us, Accessed by October 15, 2018.
2. https://www.washingtonpost.com/news/energy-environment/wp/2016/08/16/white-house-sets-new-fuel-efficiency-standards-for-heavy-duty-trucks-vans-and-buses/?noredirect=on&utm_term=.b8670498d26d , Accessed by October 15, 2018.
3. Gao, Z., Smith, D.E., Daw, C.S., Edwards, K.D., Kaul, B.C., Domingo, N. et.al., The evaluation of developing vehicle technologies on the fuel economy of long-haul trucks. Energy conversion and management, 106: 766-781, 2015.
4. Gao, Z., Lin, Z., and Franzese, O., Energy Consumption and cost savings of truck electrification for heavy-duty vehicle applications, Transportation Research Record: Journal of the Transportation Research Board, 2628: 99-109, 2017.
5. Gao, Z., Lin, Z., LaClair, T.J., Liu, C., Li, J.M., Birky, A.K. et.al., Battery capacity and recharging needs for electric buses in city transit service, Energy, 122: 588-600, 2017.
6. https://aceee.org/sites/default/files/super-truck-0517.pdf , Accessed by October 15, 2018.
7. Gao, Z., Chakravarthy, V.K., Daw, C.S., Comparisons of the simulated emissions and fuel efficiencies of diesel and gasoline hybrid electric vehicles, Proc. IMechE - Part D: Journal of Automobile Engineering, 225(7):944-959, 2011.
8. Johnson, T.V., Review of diesel emissions and control, International Journal of Engine Research, 10(5):275-285, 2009.
9. Chen, H.Y., Mulla, S., Weigert, E., Camm, K., Ballinger, T., Cox, J. et.al., Cold start concept (CSC™) a novel catalyst for cold start emission control, SAE International Journal of Fuels and Lubricants, 6(2), 372-381, 2013.
10. Gao, Z., Curran, S.J., Parks, J.E., Smith, D.E., Wagner, R.M., Daw, C.S., Thomas, J.F., Drive cycle simulation of high efficiency combustions on fuel economy and exhaust properties in light-duty vehicles. Applied Energy, 157: 762-776, 2015.
11. https://www.arb.ca.gov/msprog/onrdiesel/onrdiesel.htm, Accessed by October 15, 2018.
12. https://www.autonomie.net/, Accessed by October 15, 2018.
13. https://www.delphi.com/sites/default/files/inline-files/2016-2017-heavy-duty-amp-off-highway-vehicles_0.pdf?sfvrsn=0.03636262961639791&status=Temp, Accessed by October 15, 2018.
14. Gao, Z., Conklin, J.C., Daw, C.S., & Chakravarthy, V.K., A proposed methodology for estimating transient engine-out temperature and emissions from steady-state maps. International Journal of Engine Research, 11(2): 137-151, 2010.
15. Gao, Z., Daw, C. S., Chakravarthy, V.K., Simulation of catalytic oxidation and selective catalytic NOx reduction in lean-exhaust hybrid vehicles, SAE Technical Paper 2012-01-1304, 2012.
16. Triana, A.P., Development of models to study the emissions, flow, and kinetic characteristics from diesel oxidation catalysts and particulate filters, Dissertation, Michigan Technological University, 2005.
17. Prikhodko, V., Curran, S., Barone, T., Lewis, S. et al., Emission characteristics of a diesel engine operating with in-cylinder gasoline and diesel fuel blending, SAE Int. J. Fuels Lubr., 3(2):946-955, 2010, doi:10.4271/2010-01-2266.
18. Daw, C.S., Gao, Z., Smith, D.E., Laclair, T.J., Pihl, J.A., Edwards, K.D., Simulated fuel economy and emissions performance during city and interstate driving for a heavy-duty hybrid truck. SAE International Journal of Commercial Vehicles, 6: 161-182, 2013.
19. Gao, Z., Pihl, J.A., Parks II, J.E., Daw, C.S., 1D Kinetic Modeling of NH3-SCR with Two-Sites of NH3-Storage and Its application in LD Vehicle Emissions Control, CLEERS, 2017.
20. Gao, Z., Daw, C.S., Wagner, R.M., Edwards, K.D., & Smith, D.E., Simulating the impact of premixed charge compression ignition on light-duty diesel fuel economy and emissions of particulates and NOx. Proceedings of the Institution of Mechanical Engineers, Part D: Journal of Automobile Engineering, 227(1): 31-51, 2013.
21. Smith, D., Curran, S., Gao, Z., Powertrain controls optimization for heavy duty line haul trucks, 2015 U.S. DOE Hydrogen Program and Vehicle Technologies Program Annual Merit Review and Peer Evaluation Meeting, June 8-12, 2015, Washington DC.
22. https://www.dieselnet.com/standards/#eu, Accessed by October 15, 2018.
23. Gao, Z., Finney, C., Daw, C., LaClair, T. et al., Comparative study of hybrid powertrains on fuel saving, emissions, and component energy loss in HD trucks, *SAE Int. J. Commer. Veh.*, 7(2):414-431, 2014, https://doi.org/10.4271/2014-01-2326.
24. Gao, Z., LaClair, T.J., Smith, D.E., and Daw, C.S., Exploring fuel-saving potential of long-haul truck hybridization, Transportation Research Record: Journal of the Transportation Research Board, 2502: 99-107, 2015.

Contact Information

Zhiming Gao
Oak Ridge National Laboratory
P.O. Box 2008
Oak Ridge, TN 37831
Email: gaoz@ornl.gov
Telephone: (865) 341-1339

Acknowledgments

This work was sponsored by the U.S. Department of Energy's Vehicle Technologies office. The authors thank our colleagues for their helpful suggestions and insights in this work. The thanks also to the organizers and reviewers for their support and volunteered time.

Notice: this manuscript has been authored by UT-Battelle, LLC under Contract No. DE-AC05-00OR22725 with the U.S. Department of Energy. The United States Government retains and the publisher, by accepting the article for publication, acknowledges that the United States Government retains a non-exclusive, paid-up, irrevocable, world-wide license to publish or reproduce the published form of this manuscript, or allow others to do so, for United States Government purposes. The Department of Energy will provide public access to these results of federally sponsored research in accordance with the DOE Public Access Plan.

Appendix: The Fuel Consumption Engine Map for the commercial 2010-certificated 15-L Cummins diesel engine with the Reduced Data (In Unit of g/s)

N-m/RPM	600	700	800	900	1000	1100	1200	1300	1400	1500	1600	1700	1800	1900	2000	2100	2200
0	0.355	0.365	0.530	0.625	0.693	0.830	0.916	1.100	1.316	1.407	1.795	2.196	2.234	2.550	3.070	3.762	4.442
48	0.497	0.552	0.704	0.817	0.915	1.073	1.195	1.388	1.602	1.767	2.155	2.523	2.613	2.924	3.459	4.086	4.771
97	0.624	0.735	0.879	1.008	1.133	1.324	1.476	1.679	1.895	2.143	2.529	2.871	3.011	3.327	3.883	4.422	5.115
145	0.750	0.906	1.064	1.211	1.352	1.591	1.752	1.976	2.198	2.518	2.911	3.254	3.415	3.734	4.311	4.797	5.491
194	0.879	1.071	1.269	1.440	1.593	1.870	2.015	2.283	2.503	2.892	3.295	3.658	3.830	4.156	4.690	5.218	5.907
242	1.011	1.233	1.483	1.688	1.863	2.110	2.283	2.579	2.830	3.255	3.682	4.045	4.263	4.611	5.100	5.672	6.361
291	1.145	1.395	1.688	1.929	2.110	2.322	2.546	2.874	3.171	3.611	4.068	4.445	4.699	5.097	5.579	6.191	6.844
339	1.282	1.556	1.858	2.119	2.325	2.528	2.789	3.188	3.494	3.971	4.449	4.866	5.139	5.611	6.132	6.745	7.334
388	1.420	1.708	1.996	2.248	2.510	2.737	3.016	3.528	3.789	4.336	4.815	5.294	5.618	6.129	6.680	7.258	7.802
436	1.557	1.865	2.137	2.363	2.693	2.965	3.263	3.853	4.078	4.696	5.174	5.675	6.116	6.653	7.187	7.671	8.240
485	1.696	2.044	2.306	2.505	2.905	3.219	3.577	4.099	4.441	5.019	5.534	6.047	6.596	7.172	7.662	8.064	8.671
533	1.840	2.240	2.512	2.724	3.154	3.493	3.888	4.371	4.790	5.359	5.888	6.417	7.062	7.679	8.157	8.520	9.128
582	1.989	2.438	2.739	2.946	3.398	3.771	4.197	4.670	5.117	5.715	6.249	6.793	7.517	8.187	8.686	9.031	9.625
630	2.141	2.618	2.951	3.153	3.657	4.054	4.507	4.987	5.430	6.080	6.617	7.203	7.987	8.713	9.254	9.577	10.161
679	2.298	2.797	3.102	3.392	3.950	4.358	4.819	5.299	5.769	6.416	6.984	7.613	8.482	9.270	9.867	10.167	10.733
727	2.508	2.976	3.241	3.613	4.235	4.641	5.132	5.619	6.125	6.745	7.357	8.011	8.986	9.857	10.473	10.760	11.333
776	2.765	3.165	3.396	3.813	4.432	4.883	5.450	5.943	6.480	7.081	7.758	8.421	9.476	10.433	11.057	11.373	11.956
824	2.996	3.363	3.622	4.061	4.644	5.104	5.781	6.259	6.840	7.413	8.180	8.906	9.979	10.987	11.638	11.991	12.592
873	3.130	3.506	3.872	4.366	4.912	5.385	6.086	6.578	7.198	7.760	8.556	9.374	10.482	11.497	12.160	12.569	13.228
921	3.197	3.597	4.109	4.673	5.193	5.685	6.342	6.900	7.534	8.155	8.943	9.806	10.956	11.969	12.620	13.109	13.862
970	3.280	3.686	4.317	4.952	5.441	5.957	6.614	7.204	7.892	8.553	9.373	10.246	11.401	12.418	13.046	13.611	14.499
1018	3.432	3.839	4.516	5.198	5.677	6.213	6.917	7.497	8.283	8.941	9.845	10.772	11.850	12.837	13.436	14.085	15.167
1067	3.627	4.026	4.728	5.459	5.923	6.487	7.247	7.805	8.707	9.314	10.308	11.312	12.302	13.235	13.832	14.581	15.756
1115	3.822	4.204	4.954	5.744	6.216	6.799	7.545	8.223	9.066	9.741	10.758	11.834	12.763	13.656	14.295	15.231	15.756
1164	3.989	4.406	5.190	6.003	6.534	7.113	7.863	8.650	9.413	10.166	11.188	12.297	13.177	14.060	14.818	16.365	15.756
1212	4.164	4.627	5.437	6.258	6.839	7.420	8.187	9.075	9.767	10.561	11.583	12.632	13.504	14.320	15.223	17.593	15.756
1261	4.336	4.831	5.695	6.511	7.126	7.724	8.502	9.493	10.108	10.948	11.961	12.937	13.799	14.614	15.441	17.840	15.756
1309	4.482	5.058	5.972	6.716	7.389	8.032	8.831	9.810	10.468	11.361	12.361	13.264	14.154	15.052	15.899	17.840	15.756
1357	4.540	5.244	6.277	6.865	7.645	8.333	9.133	10.101	10.871	11.818	12.804	13.634	14.524	15.486	16.363	17.840	15.756
1406	4.540	5.244	6.554	6.953	7.922	8.617	9.404	10.426	11.259	12.300	13.293	14.060	14.895	15.892	16.713	17.840	15.756
1454	4.540	5.244	6.713	7.092	8.215	8.883	9.657	10.799	11.613	12.795	13.798	14.515	15.305	16.407	16.713	17.840	15.756
1503	4.540	5.244	6.869	7.368	8.405	9.170	9.961	11.168	11.945	13.287	14.272	14.980	15.778	16.994	16.713	17.840	15.756
1551	4.540	5.244	6.869	7.598	8.624	9.499	10.356	11.474	12.395	13.703	14.714	15.430	16.228	17.556	16.713	17.840	15.756
1600	4.540	5.244	6.869	7.802	8.908	9.861	10.740	11.828	12.828	14.112	15.136	15.840	16.646	18.137	16.713	17.840	15.756
1648	4.540	5.244	6.869	7.901	9.249	10.236	11.084	12.215	13.184	14.532	15.554	16.274	17.139	18.734	16.713	17.840	15.756
1697	4.540	5.244	6.869	7.901	9.470	10.572	11.393	12.595	13.445	14.950	15.963	16.741	17.719	18.799	16.713	17.840	15.756
1745	4.540	5.244	6.869	7.901	9.470	10.847	11.744	12.823	13.724	15.271	16.331	17.204	18.253	18.799	16.713	17.840	15.756
1794	4.540	5.244	6.869	7.901	9.470	11.114	12.067	13.041	14.103	15.541	16.657	17.630	18.736	18.799	16.713	17.840	15.756
1842	4.540	5.244	6.869	7.901	9.470	11.385	12.384	13.288	14.472	15.863	16.975	18.042	18.871	18.799	16.713	17.840	15.756
1891	4.540	5.244	6.869	7.901	9.470	11.670	12.720	13.555	14.847	16.242	17.337	18.454	18.871	18.799	16.713	17.840	15.756
1939	4.540	5.244	6.869	7.901	9.470	11.990	13.022	13.907	15.243	16.642	17.721	18.834	18.871	18.799	16.713	17.840	15.756
1988	4.540	5.244	6.869	7.901	9.470	12.318	13.340	14.306	15.645	17.004	18.083	18.834	18.871	18.799	16.713	17.840	15.756
2036	4.540	5.244	6.869	7.901	9.470	12.652	13.692	14.673	16.036	17.370	18.433	18.834	18.871	18.799	16.713	17.840	15.756
2085	4.540	5.244	6.869	7.901	9.470	12.990	14.071	14.981	16.399	17.691	18.447	18.834	18.871	18.799	16.713	17.840	15.756
2133	4.540	5.244	6.869	7.901	9.470	13.135	14.328	15.260	16.435	17.691	18.447	18.834	18.871	18.799	16.713	17.840	15.756